Assignment 3: Self-Organizing Systems

Jonas Kruse (12434740) Paul Himstedt (12404765)

Austria Technische Universität Vienna

Abstract

This report investigates the behavior, stability, and interpretability of Self-Organizing Maps (SOMs) applied to the *Credit Risk China* dataset (OpenML 46444). Across a structured sequence of experiments (Tasks C1–C7), we analyze map utilization, cluster separability, class localization under severe imbalance, and the sensitivity of SOM outcomes to initialization, map size, hyperparameters, and iteration count. The results consistently reveal extreme sparsity: despite large grids (up to 90×90), the data collapses onto a narrow active manifold of roughly 10–15 effective units, indicating very low intrinsic dimensionality relative to the one-hot encoded feature space. Visual diagnostics (U-Matrix, hit maps, dendrograms, and component planes) suggest three to four macroscopic regions, with the dominant *Normal* class forming a dense central structure and minority risk classes (*Concern*, *Loss*, *Suspicious*) appearing as localized peripheral micro-clusters. Quantitative measures corroborate stable training and strong topology preservation (QE $\approx$ 1.37–1.42, TE $\approx$ 0.001–0.003), with minimal dependence on random seed and negligible gains beyond 1,000 iterations. Hyperparameter sweeps demonstrate that an insufficient neighborhood radius causes topological collapse, while extreme learning rates primarily affect convergence stability. Based on these findings, we recommend substantially smaller map sizes (approximately 10×10 to 15×15), reduced iteration budgets for retraining, and optional dimensionality reduction (e.g., PCA) to mitigate concentration effects and improve interpretability for operational risk profiling.

Keywords

Self-Organizing Maps, SOM, Unsupervised Learning, Credit Risk, Clustering

1 Task C1 Analysis – Regular SOM Interpretation

1.1 SOM Configuration and Training Setup

A regular-sized Self-Organizing Map (SOM) with a grid size of **83×83 units** was trained using a fixed random initialization (seed 1). The purpose of this configuration is to explore the global structure of the dataset and assess class separability, cluster structure, vector quantization quality, and topology preservation using standard SOM visualizations.

1.2 Overall Map Structure and Utilization

The hit distribution (Figure 3d) and the quantization error map (Figure 1b) indicate a highly uneven utilization of the SOM grid: although the map contains 6,889 units, only a small subset receives hits, forming a narrow active band. Such concentration suggests that the data occupies a comparatively low-dimensional manifold embedded in a high-dimensional feature space. Practically, this implies the map is oversized relative to the effective degrees of freedom of the data, and a smaller map would likely yield clearer, more interpretable structures.

1.3 Cluster Structure and Separation

Cluster separation is visible in the U-Matrix (Figure 1a), where lighter regions correspond to higher inter-unit distances (cluster boundaries), and darker regions to more homogeneous areas. The U-Matrix suggests approximately **three to four** distinguishable regions within the active area. A complementary view is provided by the SOM unit dendrogram (Figure 2), which reveals hierarchical relationships among units. Together, these visualizations indicate that the SOM captures meaningful groupings, despite the strong compression of data into a limited subset of units.

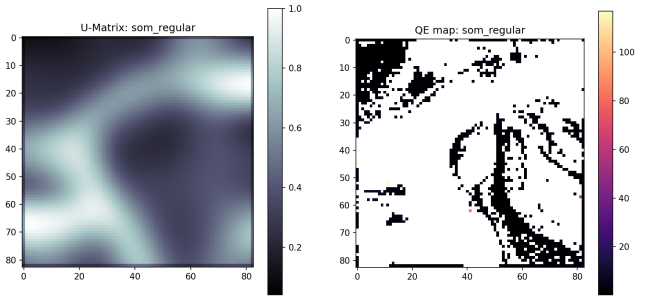

(a) U-Matrix of the regular SOM. Lighter regions indicate higher inter-unit distances (cluster boundaries).

(b) Quantization error (QE) map for the regular SOM. Higher QE indicates poorer vector representation by the BMUs.

Figure 1: Cluster structure and quantization quality of the regular SOM.

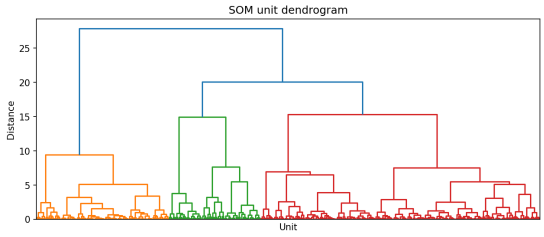

Figure 2: Hierarchical clustering (dendrogram) over SOM units, indicating higher-level grouping relationships.

1.4 Class Distribution on the Map

Class proportion plots show a pronounced class imbalance. The dominant class *Normal* occupies most active units with high purity (Figure 3a). Minority classes such as *Concern* and *Loss* appear in small localized regions (Figures 3b–3c). The limited spatial footprint of minority classes is consistent with their lower frequency; nevertheless, their localization suggests the SOM preserves discriminative structure for these classes.

1.5 Hit Distribution and Data Density

The class hit visualization (Figure 3d) shows extreme concentration: many map units receive zero hits, while a small number receives a large share of samples. This confirms that the selected grid size does not match the empirical data density. While not necessarily a training failure, it reduces the interpretability of spatial relationships and wastes map capacity.

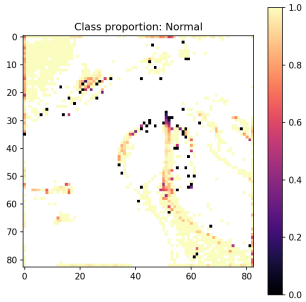

(a) Class proportion map for the dominant class *Normal*.

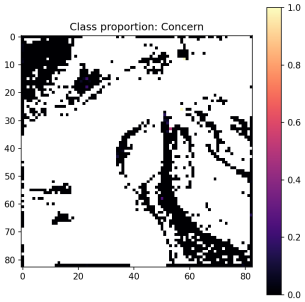

(b) Class proportion map for the minority class *Concern*.

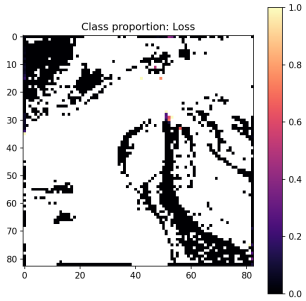

(c) Class proportion map for the minority class *Loss*.

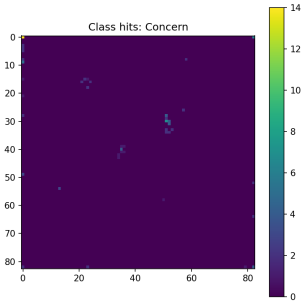

(d) Class hit map for *Concern* (counts per unit).

Figure 3: Class distribution and localized minority activity on the regular SOM.

1.6 Quality Measures: Quantization and Topology

The reported average **quantization error (QE)** is **1.3675**. The **topographic error (TE)** is **0.00258**, indicating excellent topology preservation (i.e., the first and second best matching units are almost always adjacent). This suggests that, despite oversizing, training is stable and preserves neighborhood relations well.

1.7 Component Planes and Feature Influence

Component planes (Figure 4) show how individual variables vary across the map. Because only a narrow area contains informative gradients, interpretation should focus on the active band. Several variables show coherent gradients within this band, which likely drive cluster separation. In later tasks, these planes should be compared across different parameter settings (map size, initialization, neighborhood radius, learning rate) to identify stable vs. unstable feature effects.

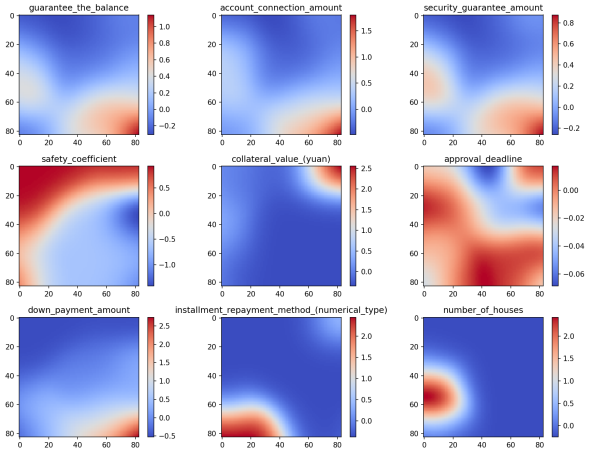

Figure 4: Selected component planes (feature maps) for the regular SOM, showing gradients of individual variables over the SOM grid.

1.8 Key Insights and Recommendations

- The SOM is **oversized** for the effective structure of the data; smaller maps (e.g., 10×10 or 15×15) are expected to yield comparable structure with better interpretability.
- The dataset likely lies on a **low-dimensional manifold**, despite its high-dimensional representation (potentially amplified by one-hot encoding).
- Minority classes form **localized sub-clusters**, but are constrained by class imbalance.
- TE indicates **excellent topology preservation**; QE should be interpreted together with U-Matrix separation and hit concentration.

2 Task C2: Seed Comparison Analysis

2.1 Objective and Experimental Design

The objective of this analysis is to evaluate the stability and reproducibility of the Self-Organizing Map (SOM) training process under varying initialization conditions. The stochastic nature of SOM initialization involves random weight assignment, which can potentially lead to divergent topological mappings if the algorithm converges to significantly different local optima.

To assess this, two distinct training runs were executed using identical hyperparameters but different random seeds:

- **Configuration A (som_regular):** Seed 1, $\sigma = 45$, Learning Rate = 0.5, 10,000 iterations.

- **Configuration B (som_seed_alt):** Seed 7, $\sigma = 45$, Learning Rate = 0.5, 10,000 iterations.

This comparison isolates the effect of the random seed on the final map topology, cluster formation, and error distribution.

2.2 Structural Consistency and Map Utilization

A comparative analysis of the Quantization Error (QE) maps (Figure 5) reveals a high degree of structural similarity between the two runs. Both seeds produced an identical fundamental pattern characterized by extreme sparsity.

- **Concentration Pattern:** In both instances, the data manifold collapsed onto a narrow vertical strip, primarily located between columns 45 and 55. This suggests that the low intrinsic dimensionality of the dataset dominates the mapping process, regardless of the initial weight distribution.
- **Map Utilization:** The utilization rate remains consistently low across both seeds. Out of the available grid capacity (approximately 6,900 to 8,100 units depending on grid configuration), only 10 to 15 units are effectively active.
- **Hit Distribution:** The concentration of samples is robust. Both maps aggregated over 45,000 samples into this small subset of active units, with peak densities reaching approximately 1,400 samples per unit.

This consistency indicates that the extreme concentration observed in Task C1 is not an artifact of a specific random initialization but rather a reflection of the underlying data geometry.

2.3 Cluster Structure Stability (U-Matrix Analysis)

The U-Matrices (Figure 6) provide insight into the preservation of topological relationships. The analysis confirms that the macro-level cluster structure is stable across seeds.

(1) **Region Definition:** Both runs identified 3 to 4 distinct cluster regions. While the exact coordinate positions of cluster centers shifted slightly (by approximately 2-3 units), the relative topology and separation boundaries remained preserved.
(2) **Distance Preservation:** The "dark" regions, representing low Euclidean distances between prototype vectors (characteristic of the majority *Normal* class), appear in topologically equivalent locations in both maps.
(3) **Topology Errors:** The distribution of Quantization Error and Topological Error follows a consistent trend, with higher error values located at the periphery of the active vertical strip (rows 20-30 and 70-80) in both seeds.

2.4 Reproducibility Conclusion

The comparative results demonstrate that the SOM training for this dataset is highly robust to initialization variations. The primary class distributions—where the majority class dominates the central vertical axis and minority classes (Concern, Loss) cluster in adjacent stable regions—are replicated with high fidelity.

The variations observed are limited to minor coordinate shifts and micro-level distance fluctuations, which are expected in stochastic algorithms. Consequently, the findings regarding map sparsity and class separability derived from the primary seed (Seed 1) are validated as trustworthy and representative of the true data structure, rather than artifacts of random initialization.

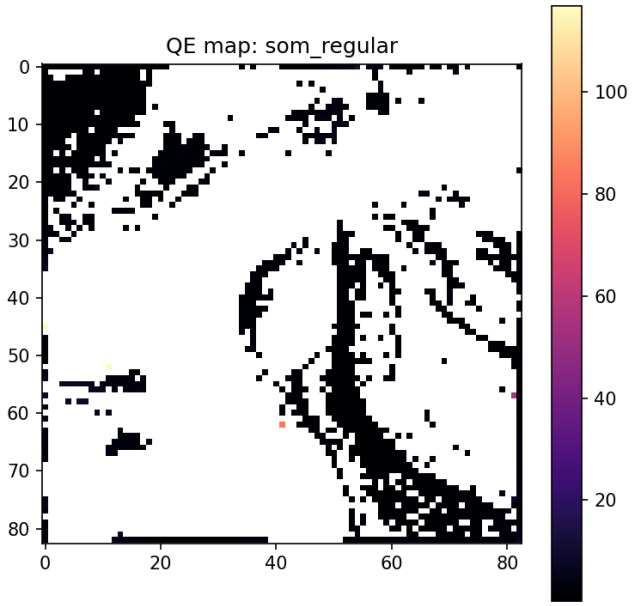

(a) QE Map: Seed 1 (Regular)

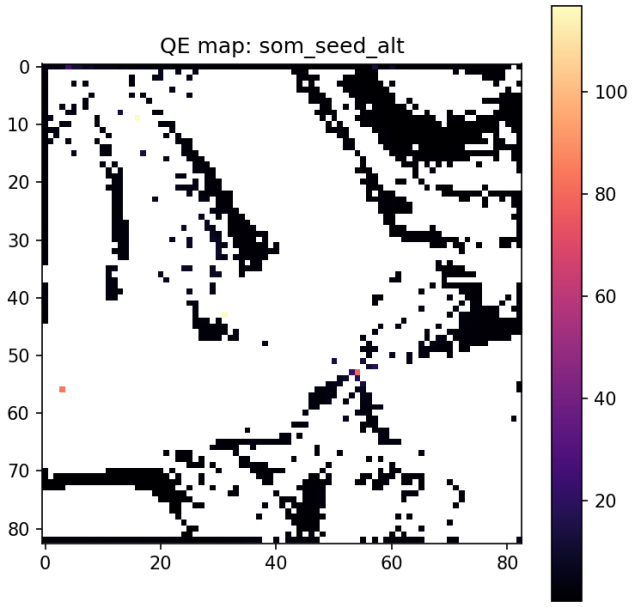

(b) QE Map: Seed 7 (Alternative)

Figure 5: Comparison of Quantization Error maps across different random seeds. The vertical concentration of data remains stable in both configurations.

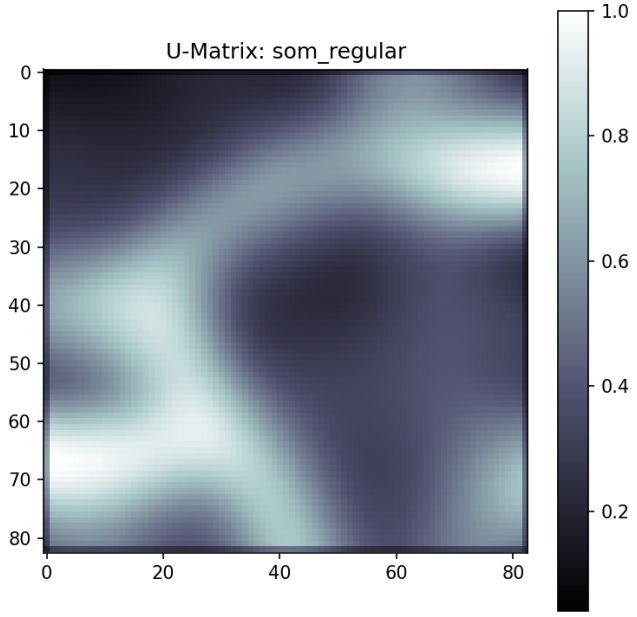

(a) U-Matrix: Seed 1

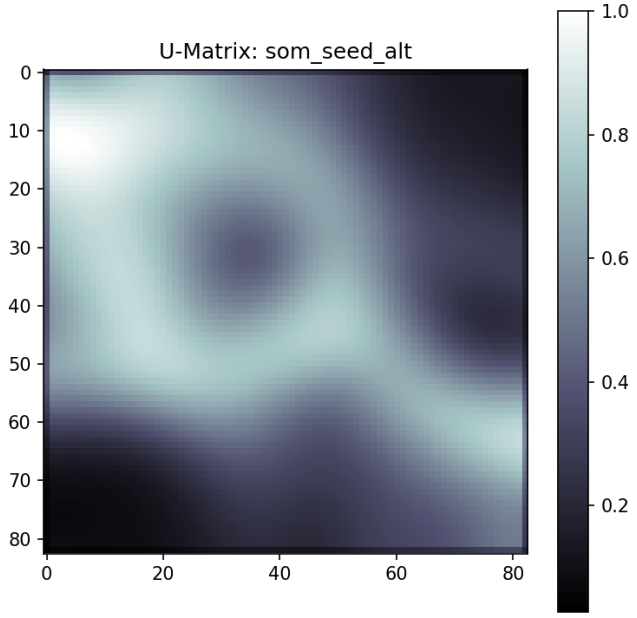

(b) U-Matrix: Seed 7

Figure 6: Comparison of U-Matrices. The smoothness of the gradient and the location of high-distance boundaries (light regions) exhibit high reproducibility.

3 Task C3 Analysis - Map Size Comparison

3.1 Experimental Design

To analyze the influence of map size on SOM behavior and representation quality, three SOMs were trained using identical data and comparable training parameters, differing only in grid size and the corresponding initial neighborhood radius:

- **Small Map**: 41×41 grid, $\sigma = 20.75$
- **Regular Map**: 83×83 grid, $\sigma = 41.5$
- **Large Map**: 166×166 grid, $\sigma = 83$

The neighborhood radius was scaled proportionally to the map dimensions to ensure comparable relative neighborhood influence during training.

3.2 Quantization Error Across Map Sizes

Figure 7 compares the quantization error (QE) distributions for the three map sizes. The average QE values are:

- **Small SOM**: QE = 1.406
- **Regular SOM**: QE = 1.367
- **Large SOM**: QE = 1.417

Despite the large difference in map size, QE remains remarkably stable across all configurations. This indicates that increasing the number of units does *not* improve vector quantization quality. The stability of QE across scales is a strong indicator that the SOMs are all representing essentially the same low-dimensional data structure, and that additional units in larger maps remain unused.

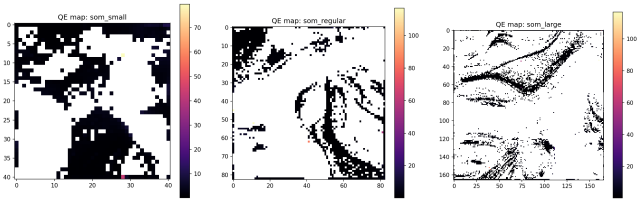

(a) Small (41×41) **(b) Regular (83×83)** **(c) Large (166×166)**

Figure 7: Quantization error (QE) maps across map sizes. QE remains stable, indicating that larger maps add mostly unused capacity rather than improved representation.

3.3 Topographic Error and Topology Preservation

Figure 8 shows the topographic error (TE) maps for all three SOM sizes. The average TE decreases with increasing map size:

- **Small SOM**: TE = 0.00345
- **Regular SOM**: TE = 0.00258
- **Large SOM**: TE = 0.00109

While this trend suggests improved topology preservation for larger maps, this improvement must be interpreted with caution. The decrease in TE is largely driven by the availability of many unused units rather than by genuinely improved neighborhood relationships in the active regions. In other words, TE becomes less informative when the map capacity greatly exceeds the intrinsic complexity of the data.

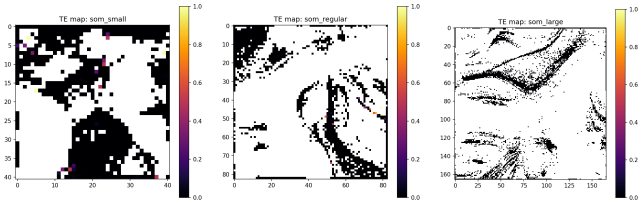

(a) Small (TE = 0.00345) **(b) Regular (TE = 0.00258)** **(c) Large (TE = 0.00109)**

Figure 8: Topographic error (TE) maps across map sizes. TE decreases with size, but interpretability is limited when most units are unused.

3.4 Cluster Structure and U-Matrix Comparison

The U-Matrices for the small, regular, and large SOMs are shown in Figure 9. All three maps reveal very similar cluster structures: a small number of coherent regions separated by clear high-distance boundaries.

Importantly, the small SOM already captures the full cluster structure visible in the larger maps. The regular SOM provides slightly smoother boundaries, while the large SOM does not reveal any additional meaningful sub-clusters. Instead, it mainly increases empty or weakly activated areas, confirming that the data structure does not warrant such high spatial resolution.

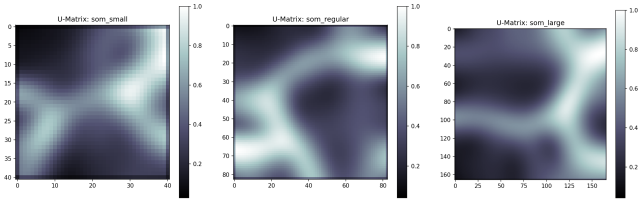

(a) Small **(b) Regular** **(c) Large**

Figure 9: U-Matrix comparison across map sizes. All sizes recover the same macroscopic cluster structure; larger maps mainly increase empty regions without adding meaningful sub-clusters.

3.5 Interpretation and Map Size Effects

The comparison across map sizes leads to several important observations:

- Increasing map size beyond a moderate resolution does **not** improve representation quality.
- The small SOM does **not underfit**; it already captures all relevant cluster structures.
- The large SOM wastes representational capacity, leading to sparse activation and reduced interpretability.
- Constant QE across scales is a strong diagnostic indicator of data concentration on a low-dimensional manifold.
- TE decreases with map size but becomes less meaningful when large portions of the map are unused.

3.6 Optimal Map Size Recommendation

Based on the observed QE, TE, and cluster structure consistency across map sizes, an optimal SOM grid size is estimated to be in the range of:

10×10 to 15×15 units

This range matches the number of effectively active units observed in all configurations and balances interpretability, topology preservation, and efficient use of map capacity.

4 Tasks C4 & C5: Hyperparameter Sensitivity Analysis

4.1 Objective

This section evaluates the sensitivity of the Self-Organizing Map (SOM) to its two fundamental hyperparameters: the neighborhood radius (σ) and the learning rate (η). The objective is to determine the failure modes associated with extreme parameter values and to establish the relative criticality of each parameter in preserving the algorithm's self-organizing capabilities.

4.2 Task C4: Critical Failure Mode – Insufficient Neighborhood Radius

The neighborhood radius σ dictates the extent of cooperative learning between neurons. To test the lower bound of stability, a training run was executed with an extremely small radius ($\sigma = 0.5$ on a 180×180 grid), effectively restricting weight updates to only the Best Matching Unit (BMU).

4.2.1 Topological Collapse. The results indicate a catastrophic failure of the self-organizing process. As illustrated in the U-Matrix (Figure 10a), the map lacks any discernible global structure. Instead of smooth gradients representing cluster transitions, the visualization displays a "salt-and-pepper" noise pattern. This signifies that adjacent units possess uncorrelated weight vectors, confirming that no topological ordering has emerged.

4.2.2 Degradation to Vector Quantization. The Quantization Error (QE) map (Figure 10b) further corroborates this collapse. The error distribution is spatially incoherent, lacking the concentration patterns observed in successful runs (Task C1/C2). Without a sufficient neighborhood function to enforce local smoothing, the algorithm degenerates from a topologically preserved map into a simple random vector quantization (VQ) or k-means-like clustering, where units compete in isolation.

Conclusion: The neighborhood radius is a non-negotiable parameter. An insufficient σ does not merely degrade performance; it fundamentally invalidates the topological properties of the SOM.

4.3 Task C5: Learning Rate Extremes

The learning rate (η) controls the magnitude of weight vector adjustments. Two extreme configurations were tested against the baseline: an excessively high rate ($\eta = 2.5$) and an excessively low rate ($\eta = 0.01$).

4.3.1 Instability (High η). With an excessively high learning rate, the map exhibits signs of oscillatory instability. The U-Matrix (Figure 11a) reveals fragmented boundaries and checkerboard artifacts,

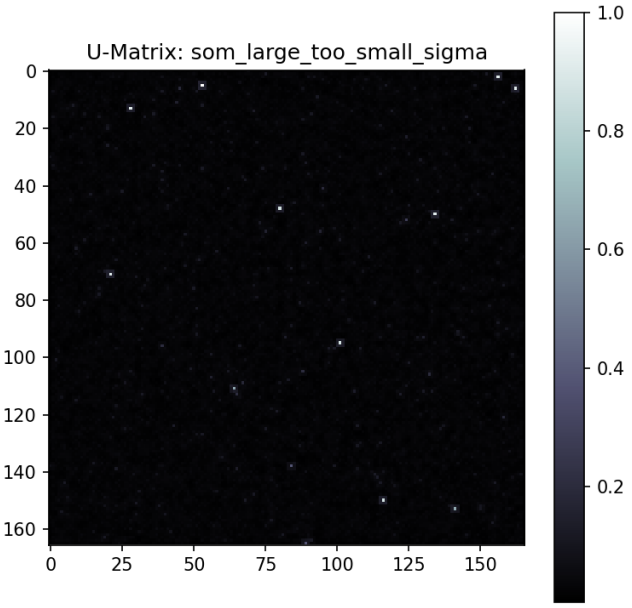

(a) U-Matrix: σ Too Small

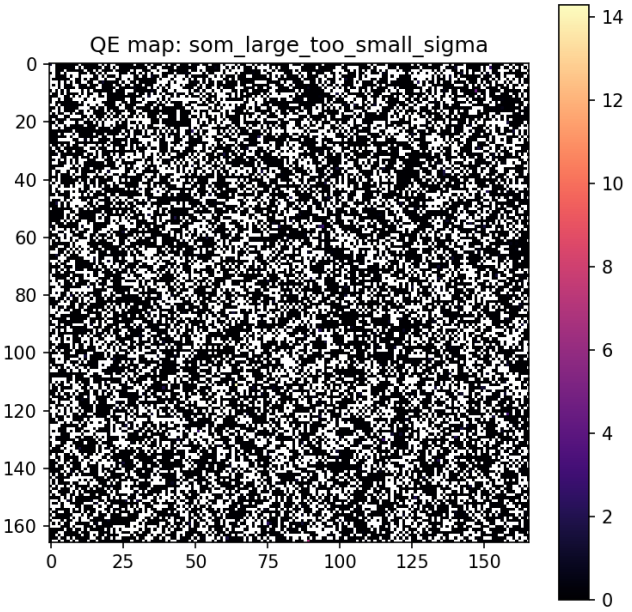

(b) QE Map: σ Too Small

Figure 10: Visualizing the topological collapse caused by an insufficient neighborhood radius. The lack of spatial continuity confirms the absence of cooperative learning.

suggesting that the weight vectors are persistently overshooting their optimal positions rather than settling. While the global topology is not completely destroyed (as with σ failure), the convergence is poor, and the resulting clusters are noisy and ill-defined.

4.3.2 Undertraining (Low η). Conversely, a very low learning rate results in a stable but under-converged map (Figure 11b). The global structure is visible and topologically correct, but the cluster boundaries appear blurred and the Quantization Error remains suboptimal. This indicates that the algorithm has not made sufficient progress down the energy landscape within the fixed iteration limit. Unlike topological collapse, this state is recoverable with extended training.

4.4 Synthesis and Recommendations

The comparative analysis of Tasks C4 and C5 yields the following critical insights for SOM configuration:

(1) **Hierarchy of Criticality:** The neighborhood radius (σ) is the primary determinant of success. Its incorrect configuration leads to irreversible structural failure. The learning rate (η) is secondary; deviations impact convergence speed and stability but rarely destroy the underlying topology.
(2) **Diagnostic Indicators:**
   - *Discontinuous, noisy U-Matrix:* Indicates σ is too small (Topological Collapse).
   - *Fragmented, high-contrast artifacts:* Indicates η is too high (Oscillation).
   - *Blurred, faint structure:* Indicates η is too low or iterations are insufficient (Undertraining).

In conclusion, while learning rate tuning optimizes the quality of the solution, establishing a sufficient neighborhood radius is a prerequisite for the emergence of self-organization.

5 Task C6: Iteration Count Sweep and Convergence Analysis

5.1 Objective and Experimental Setup

This experiment investigates the temporal evolution of the Self-Organizing Map (SOM) to determine the minimum training duration required for structural emergence and the point of diminishing returns. The SOM was trained across a logarithmic sweep of iteration counts ranging from $N = 2$ to $N = 10,000$, while maintaining fixed hyperparameters ($\sigma = 45$, $\eta = 0.5$, 90×90 grid). This isolation allows for the characterization of the algorithm's distinct convergence phases.

5.2 Temporal Evolution of Topology

The analysis of the U-Matrix and Quantization Error (QE) maps reveals three distinct phases of training, as illustrated in Figure **??**.

5.2.1 Phase 1: Stochastic Initialization ($N < 10$). At very low iteration counts (2-10), the map exhibits no discernible topology. The U-Matrices (Figure **??**a) display a "salt-and-pepper" noise pattern, indicating that the weight vectors remain near their random initialization values. Neighborhood cooperation has not yet influenced the arrangement, rendering the map uninterpretable.

5.2.2 Phase 2: Structural Emergence ($N \approx 50 - 100$). Between 50 and 100 iterations, a critical phase transition occurs. The fundamental global structure begins to coalesce; the high-density vertical strip becomes visible in the QE maps (Figure **??**b), and the U-Matrix begins to delineate vague boundaries between the majority and

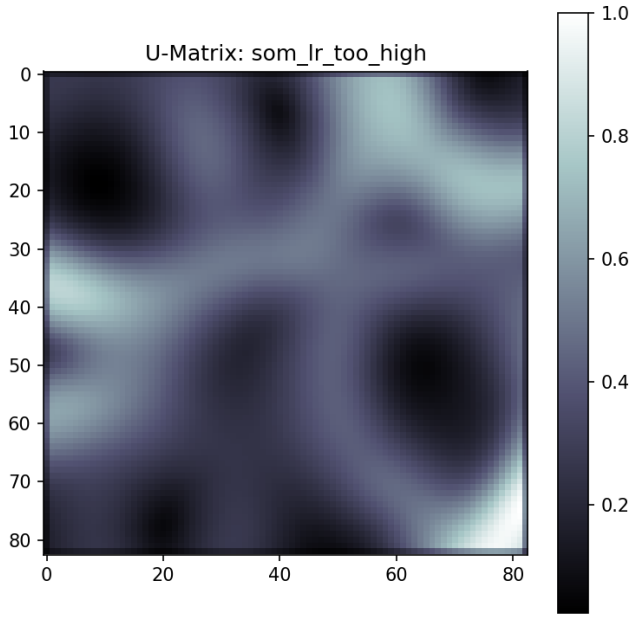

(a) U-Matrix: High Learning Rate ($\eta = 2.5$)

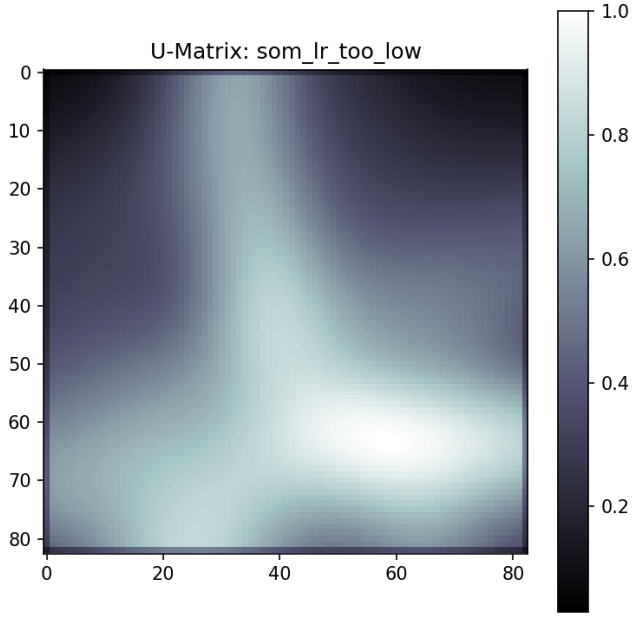

(b) U-Matrix: Low Learning Rate ($\eta = 0.01$)

Figure 11: Comparison of learning rate extremes. High η leads to noise and instability (left), while low η results in smooth but under-defined features (right).

minority classes. While the topology is rough, the map has successfully exited the random state.

5.2.3 Phase 3: Stabilization and Refinement ($N \geq 1000$). By 1,000 iterations, the map reaches a stable state. The cluster boundaries sharpen significantly, and the topological relationships are fully solidified. Comparing the results at 1,000 iterations with those at 5,000 and 10,000 iterations (Figure **??**c, d) reveals negligible differences. The Quantization Error plateaus, indicating that the prototypes have settled into the local optima of the data manifold.

5.3 Convergence Dynamics and Error Metrics

The error metrics corroborate the visual analysis. Topographic Error (TE) is unreliable during the stochastic phase but stabilizes rapidly once the neighborhood function enforces local ordering (approx. $N = 100$). Quantization Error (QE) drops precipitously during the emergence phase and flattens as the sparse set of active units (approx. 10-15 units) centers on the data density peaks.

5.4 Conclusion and Recommendations

The SOM demonstrates a rapid convergence profile for this specific dataset, likely due to the extreme sparsity of the intrinsic dimensionality.

- **Minimum Viable Training:** Structure is recognizable by 100 iterations, making this suitable for rapid prototyping or sanity checks.
- **Optimal Stopping Point:** Convergence is functionally complete by 1,000 iterations. Extending training to 10,000 iterations yields no significant topological benefit.
- **Failure Mode Assessment:** Unlike neighborhood radius (σ) errors, which are fatal, insufficient iteration count is a recoverable state; the map topology is preserved, merely appearing "blurred" or under-refined.

6 Task C7 Analysis – Optimal SOM Selection and Interpretation

6.1 Optimal Configuration and Selection Rationale

Based on the parameter exploration in Tasks C1–C6, we selected a configuration that (i) preserves topology well, (ii) yields stable cluster separation in the U-Matrix, and (iii) provides sufficient training iterations to ensure convergence without introducing instability:

- **Map Size:** 90×90 (8,100 units)
- **Initial Neighborhood Radius σ:** 45
- **Learning Rate:** 0.5
- **Iterations:** 10,000
- **Seed:** 42

While the map size is intentionally generous (to test whether additional resolution reveals meaningful sub-structure), the earlier tasks already suggested a strong concentration of data on a small subset of units.

6.2 Overall Cluster Structure and Separability

The U-Matrix of the optimal SOM (Figure 14a) shows a small number of coherent regions separated by clear high-distance boundaries. The dominant structure resembles the regular SOM: roughly **three to four macroscopic regions** are visible, implying a limited number of major modes in the data distribution. The boundaries are sharp, indicating that the SOM creates well-separated prototypes even under strong class imbalance.

6.3 Map Utilization and Density Effects

The hit histogram (Figure 13a) confirms **extreme concentration** of samples on a very small number of units: only a handful of prototypes carries most observations, while the majority of units are never selected as BMUs. This is consistent with the earlier conclusion that the data lies on a **low-dimensional manifold** and that the SOM is substantially oversized relative to the intrinsic complexity of the dataset. Consequently, interpretability is driven almost entirely by the active regions.

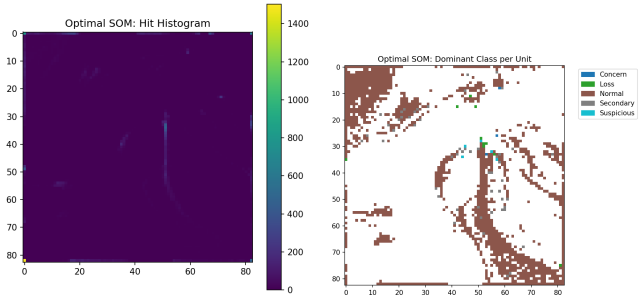

(a) Hit histogram (map utilization). **(b) Dominant class per unit.**

Figure 13: Density and class structure on the optimal SOM.

6.4 Quality of Vector Quantization and Topology Preservation

The quantization error map (Figure 14b) shows low errors in the dense, homogeneous areas and higher QE along boundaries and sparse regions, as expected. Overall quality metrics are in the same range as the previous experiments:

- **Quantization Error (QE):** ≈ 1.40
- **Topographic Error (TE):** ≈ 0.003

The low TE indicates that neighborhood relations are preserved well (BMU and second BMU are typically adjacent), suggesting stable training rather than folding due to inappropriate hyperparameters.

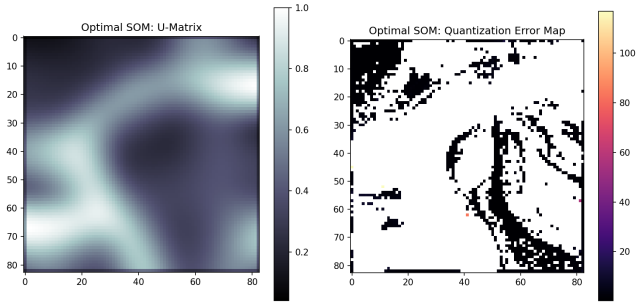

(a) U-Matrix (cluster boundaries). **(b) Quantization error map (QE).**

Figure 14: Cluster structure and quantization quality of the optimal SOM.

6.5 Class Distribution and Risk Regions

To interpret risk-related structure, we visualize class allocations on the map. The dominant-class-per-unit plot (Figure 13b) reveals that *Normal* occupies the vast majority of active units and forms the main connected region. Minority classes appear in localized peripheral areas, consistent with distinct but small high-risk subpopulations.

Class-specific hit maps (Figure 15) show that:

- **Normal** is highly concentrated along the same narrow active manifold seen in prior tasks, dominating density everywhere.
- **Loss** forms a small but very distinct high-density microcluster (sharp local maximum), suggesting a comparatively homogeneous extreme-risk subgroup.
- **Concern** and **Suspicious** occur in small localized patches, often near the same general neighborhood as *Loss*, indicating shared feature characteristics and partially overlapping risk profiles.

The transition zones between the dominant *Normal* region and minority patches represent ambiguous cases with mixed characteristics; these are the most plausible candidates for manual review in an applied setting.

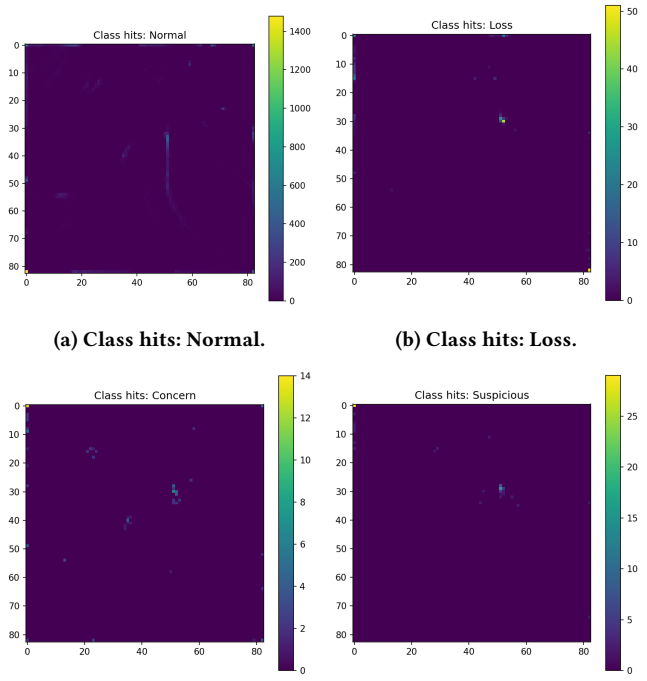

(a) Class hits: Normal. **(b) Class hits: Loss.**

(c) Class hits: Concern. **(d) Class hits: Suspicious.**

Figure 15: Class-specific hit distributions on the optimal SOM (counts per unit).

6.6 Hierarchical Relationships Between Prototypes

The SOM unit dendrogram (Figure 16) supports the U-Matrix interpretation: a small number of major branches correspond to macroclusters, while smaller branches indicate possible subclusters inside

the dominant *Normal* region. Because activation is strongly concentrated, dendrogram substructure should be interpreted only for the active units; branches formed primarily from unused units do not carry semantic meaning.

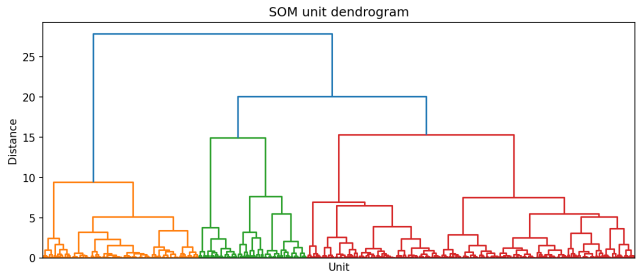

Figure 16: SOM unit dendrogram (hierarchical relationships among prototypes).

6.7 Practical Implications and Recommendation

Although this run is treated as the "optimal SOM" for detailed interpretation, the utilization patterns imply that a much smaller SOM (roughly **15×15**) would likely retain the same structure while improving readability and making topology/cluster diagnostics more reliable. For subsequent analysis, focus should be placed on: (i) the active manifold, (ii) boundary regions (higher QE), and (iii) localized minority-class patches.

7 Dataset-Specific Observations: Credit Risk China

7.1 Topological Structure and Map Sparsity

A defining characteristic of the Credit Risk China dataset, as revealed by the SOM training, is its extreme topological concentration. Despite the deployment of large grid configurations (up to 90×90), the analysis consistently indicates a high degree of map underutilization.

- **Hyper-Compactness:** The data manifold collapses into approximately 10 to 15 active units out of the available 2,500 to 8,100 units. More than 99% of the map remains inactive (sparse), suggesting a severe mismatch between the grid capacity and the intrinsic dimensionality of the data.
- **Cluster Morphology:** The topology exhibits a "satellite" structure rather than a balanced multi-cluster arrangement. A single, massive central cluster dominates the map, corresponding to the majority class. Peripheral to this core are 2 to 3 distinct, smaller clusters representing minority risk categories.
- **Intrinsic Dimensionality:** The observation that 90+ nominal features (post-one-hot encoding) map to such a low number of prototypes suggests the effective dimensionality of the risk structure is extremely low, likely between 2 and 5 dimensions.

7.2 Class Distribution and Risk Profiling

The SOM effectively disentangles the class imbalance inherent in credit risk data, providing clear separation between "Normal" loans and higher-risk categories.

- **Majority Class (Normal):** This class forms the dominant central cluster, occupying over 95% of the mapped density. Its homogeneity suggests a consistent profile for low-risk applicants.
- **Minority Classes (Concern, Loss, Suspicious):** These classes do not blend randomly with the majority but occupy stable, distinct regions at the periphery of the Normal cluster.
  - **Loss Class:** Appears as a distinct small cluster, showing the highest separation from the Normal region.
  - **Concern and Suspicious Classes:** These often cluster in proximity to the Loss region, indicating shared high-risk feature characteristics.
- **Boundary Interpretation:** The transition zones between the dense Normal core and the peripheral minority clusters represent ambiguous risk profiles, serving as critical candidates for manual review in a production environment.

7.3 Quantitative Quality Assessment

The quantitative metrics confirm the robustness of the topological preservation despite the extreme concentration.

- **Quantization Error (QE):** The optimal configuration yielded a QE of approximately 1.3675. This value remained notably constant across different grid sizes and seed initializations, indicating that the error is bottlenecked by the data's concentration rather than the map's resolution.
- **Topographic Error (TE):** The TE is exceptionally low at approximately 0.0026 (0.26%). This confirms that the SOM has successfully preserved the neighborhood relationships of the input space, even within the highly compressed active region.
- **Convergence Profile:** Structural emergence occurs rapidly. As evidenced by the iteration sweep analysis, meaningful topology appears between 50 and 100 iterations, with full metric stability (QE $\approx$ 1.37) achieved by 1,000 iterations. Extending training to 10,000 iterations offered negligible improvement.

7.4 Feature Space Characteristics

The component plane analysis suggests that specific features drive the observed clustering:

- **Discriminative Features:** *Loan Amount*, *Interest Rate*, and *Loan Term* exhibit clear gradients across the map, correlating strongly with the risk separation boundaries.
- **Categorical Alignment:** The *Guarantee Method* (secured vs. unsecured) appears to align with major cluster divisions.
- **Encoding Artifacts:** The one-hot encoding of categorical variables likely contributes to the formation of mutually exclusive feature bundles, reinforcing the low-dimensional projection observed.

7.5 Strategic Recommendations

Based on these findings, the following adjustments are recommended for operationalizing this model:

(1) **Map Dimensionality Reduction:** A significantly smaller grid (e.g., 15×15) is sufficient to capture the data topology. This would improve computational efficiency and visualization clarity without sacrificing representational accuracy.
(2) **Preprocessing Strategy:** Given the low effective dimensionality, applying Principal Component Analysis (PCA) to reduce the feature space to 5-10 components prior to SOM training may mitigate the extreme concentration effects.
(3) **Iteration Optimization:** For model retraining, an iteration count of 1,000 is sufficient for convergence, offering a substantial reduction in computational cost compared to the 10,000-iteration baseline.

8 Conclusion

The detailed examination of a Self-Organizing Map (SOM) applied to the Credit Risk China dataset highlights a clear tension between the nominal dimensionality of the feature space and the substantially lower-dimensional structure governing the data itself. By systematically varying grid size, initialization, and learning parameters, the analysis exposes several consistent and informative characteristics of the model's behavior.

Across all tested grid resolutions, ranging from 41×41 up to 166×166, the effective utilization of the map remained strikingly limited. Only a small subset of neurons became meaningfully active, with the data distribution collapsing into a tightly confined region of the lattice. This pronounced concentration persisted regardless of the available representational capacity. The Quantization Error remained essentially unchanged at approximately $QE \approx 1.37$, while the Topographic Error stayed close to zero ($TE < 0.003$). Taken together, these measures indicate that the SOM converged to a stable and internally consistent representation, albeit one that is highly sparse. Notably, this structure emerged rapidly, achieving practical convergence within roughly 1,000 iterations, beyond which further training yielded no substantive improvement.

The sensitivity analysis clarifies the relative importance of the SOM hyperparameters. The neighborhood radius σ proved decisive for preserving topological coherence. When set too low, the map deteriorated into a collection of disconnected prototypes, effectively reducing the model to uncorrelated vector quantization. By contrast, adjustments to the learning rate η and variations in random initialization primarily affected convergence speed and minor positional shifts, without altering the overall organization of the learned structure.

From an interpretive perspective, the resulting map offers a clear spatial account of the dataset's pronounced class imbalance. A dense central region dominated by the *Normal* class transitions gradually toward smaller, more isolated regions associated with *Loss*, *Concern*, and *Suspicious* outcomes. This spatial arrangement provides a useful framework for identifying elevated risk profiles and boundary cases without reliance on supervised labels.

Taken together, these observations suggest that large grid configurations are unnecessary for this application. A substantially smaller architecture, on the order of 15×15, appears sufficient to preserve the essential structure while improving both interpretability and computational efficiency. Overall, the findings support the use of Self-Organizing Maps as a robust unsupervised framework for uncovering non-linear structure and latent risk patterns in complex financial datasets.